Parametric Resonance of a Spinning Disk Under Space-Fixed Pulsating Edge Loads

Jen-San Chen
Associate Professor,
Department of Mechanical Engineering,
National Taiwan University,
Taipei, Taiwan 107

The parametric resonance of a spinning disk under a space-fixed pulsating edge load is investigated analytically. We assume that the radial edge load can be expanded in a Fourier series. With use of the orthogonality properties among the eigenfunctions of a gyroscopic system, the partial differential equation of motion is discretized into a system of generalized Hill's equations in the first-order form. The method of multiple scale is employed to determine the conditions for single mode as well as combination resonances to occur. For any two modes, with s and υ nodal diameters, respectively, combination resonance occurs only when there exists a specific Fourier component cos kθ in the edge load, where s + υ = ±k. Sum type resonance occurs when both modes are reflected or both modes are nonreflected. On the other hand, difference type resonance occurs when one mode is reflected and the other is nonreflected. In applying this rule, the number of nodal diameters of a forward and a reflected wave is considered as negative. Several typical loadings are discussed, including uniform and concentrated edge loads.

Introduction

The vibration analysis of a spinning disk under a space-fixed edge load attracts attention because of its possible application in such fields as circular saw cutting and grind wheel operation. Carlin and his co-workers' investigation (1975) appears to be the first paper attempting to calculate the natural frequencies of a spinning disk under a concentrated radial edge load. Radcliffe and Mote (1977) extended the work of Carlin et al. by considering a general concentrated edge load with both radial and tangential components. The formulations in these two papers did not take into account the effects of relative motion between the spinning disk and the space-fixed edge load. Recently Chen (1994) reformulated the problem with emphasis on the effects of relative motion between the disk and the edge load on the stability and natural frequencies of the loaded disk. He reported that both divergence and flutter instabilities are induced by the space-fixed edge load when the disk is spinning at or beyond the first critical speed.

The edge loads in these aforementioned works are assumed to be independent of time. In the case when the edge loads are periodically varying, parametric resonance may be induced. Tani and Nakamura (1978, 1980) studied the dynamic instability of an annular disk under periodically varying in-plane edge traction. The disk considered in their papers is clamped on both the inner and outer radii, and the edge traction is uniform in the circumferential direction. Zajaczkowski (1983) investigated the parametric resonance of a clamped-free disk under both uniform and concentrated pulsating torques. In these papers both the annular disk and the periodic loading are fixed in space.

A natural extension of these previous analyses is to study the dynamic instability of a spinning annular disk under periodically varying edge load which is fixed in space. This investigation may find application in the wood cutting industry as it represents a more general model for the cutting process by a circular saw. In the present paper, we first write the equation of motion for a spinning disk under a periodically varying in-plane load with arbitrary distribution on the outer rim. We assume that the edge load can be expressed as a Fourier series expansion. The resulted equation of motion is gyroscopic, and can be discretized with use of the orthogonality properties among the eigenfunctions of the unloaded disk. A system of generalized Hill's equations in the first-order form is obtained. The method of multiple scale is then employed to determine the conditions for parametric resonance to occur. Several typical forms of radial edge loads are considered, including uniform and concentrated loading.

Equation of Motion

Figure 1 shows a circular disk, which is clamped at the inner radius $r = a$ and subjected to a periodic radial traction at the outer radius $r = b$. We assume that the edge in-plane traction can be expanded in a Fourier series $\epsilon \cos \gamma t \sum_{k=0}^{\infty} f_k \cos k\theta$. ϵ has a dimension of stress, and γ is the excitation frequency of the edge load. f_k is a dimensionless scalar representing the weighting of each Fourier component. The disk is rotating with constant speed Ω, while the edge load is fixed in space. The direction of the edge load remains the same when the disk vibrates laterally. The equation of motion of the system, in terms of the transverse displacement w and with respect to the stationary coordinate system (r, θ), is

$$\rho h\left(\frac{\partial^2 w}{\partial t^2} + 2\Omega \frac{\partial^2 w}{\partial t \partial \theta} + \Omega^2 \frac{\partial^2 w}{\partial \theta^2}\right) + D\nabla^4 w + Lw + \epsilon \cos \gamma t \sum_{k=0}^{\infty} f_k \hat{L}_k w = 0 \quad (1)$$

where

$$D = \frac{Eh^3}{12(1 - \nu^2)}.$$

The parameters ρ, h, E, and ν are the mass density, thickness, Young's modulus, and Poisson ratio of the disk, respectively. L is the membrane operator associated with the axisymmetrical

Contributed by the Applied Mechanics Division of THE AMERICAN SOCIETY OF MECHANICAL ENGINEERS for publication in the ASME JOURNAL OF APPLIED MECHANICS.

Discussion on this paper should be addressed to the Technical Editor, Professor Lewis T. Wheeler, Department of Mechanical Engineering, University of Houston, Houston, TX 77204-4792, and will be accepted until four months after final publication of the paper itself in the ASME JOURNAL OF APPLIED MECHANICS.

Manuscript received by the ASME Applied Mechanics Division, Jan. 23, 1995; final revision, May 1, 1996. Associate Technical Editor: S. W. Shaw.

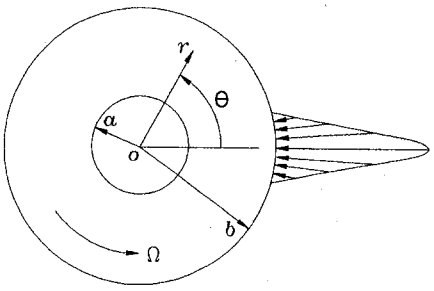

Fig. 1 A spinning disk subjected to a space-fixed pulsating edge load

stress field due to the centrifugal force, and $\hat{L}_k$ is the membrane operator associated with the stress field due to the Fourier component cos $k\theta$ of the edge traction,

$$L \equiv -\frac{h}{r}\left[\frac{\partial}{\partial r}\left(r\sigma_r\frac{\partial}{\partial r}\right)+\frac{\partial}{\partial\theta}\left(\frac{1}{r}\sigma_\theta\frac{\partial}{\partial\theta}\right)\right]$$

$$\hat{L}_k \equiv -\frac{h}{r}\left[\frac{\partial}{\partial r}\left(r\hat{\sigma}_{rk}\frac{\partial}{\partial r}+\hat{\sigma}_{r\theta k}\frac{\partial}{\partial\theta}\right)+\frac{\partial}{\partial\theta}\left(\hat{\sigma}_{r\theta k}\frac{\partial}{\partial r}+\frac{1}{r}\hat{\sigma}_{\theta k}\frac{\partial}{\partial\theta}\right)\right].$$

Stress fields σ_r and σ_θ are due to the centrifugal force and are proportional to Ω^2. On the other hand, $\hat{\sigma}_{rk}$, $\hat{\sigma}_{r\theta k}$, and $\hat{\sigma}_{\theta k}$ are the dimensionless stress fields induced by the radial edge traction cos $k\theta$ and can be expressed as

$$\hat{\sigma}_{rk}(r,\theta)=\tilde{\sigma}_{rk}(r)\cos k\theta$$

$$\hat{\sigma}_{\theta k}(r,\theta)=\tilde{\sigma}_{\theta k}(r)\cos k\theta \qquad k=0,1,2,\ldots.$$

$$\hat{\sigma}_{r\theta k}(r,\theta)=\tilde{\sigma}_{r\theta k}(r)\sin k\theta$$

$\tilde{\sigma}_{rk}$, $\tilde{\sigma}_{\theta k}$, and $\tilde{\sigma}_{r\theta k}$ are functions of radial coordinate r only, and can be found readily in Coker and Filon (1957). It is noted that $\tilde{\sigma}_r(b)=1$ and $\tilde{\sigma}_{r\theta}(b)=0$ due to the in-plane traction boundary conditions on the outer rim.

The associated boundary conditions for Eq. (1) are

$$w = w_{,r} = 0 \quad \text{at} \quad r=a \tag{2a}$$

$$B_1 w + \epsilon\cos\gamma t\sum_{k=0}^{\infty} f_k\hat{B}_{1k}w = B_2 w = 0 \quad \text{at} \quad r=b \tag{2b}$$

where the boundary operators are defined as

$$B_1 \equiv \frac{\partial}{\partial r}\left(\frac{\partial^2}{\partial r^2}+\frac{\partial}{r\partial r}+\frac{\partial^2}{r^2\partial\theta^2}\right)+\frac{1-\nu}{r^2}\left(\frac{\partial^3}{\partial r\partial\theta^2}-\frac{\partial^2}{r\partial\theta^2}\right)$$

$$\hat{B}_{1k} \equiv \frac{h\cos(k\theta)}{D}\frac{\partial}{\partial r}, \quad B_2 \equiv \frac{\partial^2}{\partial r^2}+\frac{\nu}{r}\left(\frac{\partial}{\partial r}+\frac{\partial^2}{r\partial\theta^2}\right).$$

The transverse component of the edge traction can also be included in Eq. (1), and excluded from boundary condition (2b). The equivalent boundary value problem becomes

$$\rho h\left(\frac{\partial^2 w}{\partial t^2}+2\Omega\frac{\partial^2 w}{\partial t\partial\theta}+\Omega^2\frac{\partial^2 w}{\partial\theta^2}\right)+D\nabla^4 w+Lw$$

$$+\epsilon\cos\gamma t\sum_{k=0}^{\infty} f_k\left[\hat{L}_k w+h\delta(r-b)\cos k\theta\frac{\partial w}{\partial r}\right]=0 \tag{3}$$

and

$$w = w_{,r} = 0 \quad \text{at} \quad r=a \tag{4a}$$

$$B_1 w = B_2 w = 0 \quad \text{at} \quad r=b. \tag{4b}$$

$\delta(\cdot)$ is the Dirac delta function.

It is convenient to introduce dimensionless variables (denoted with an asterisk),

$$w^* = \frac{w}{h}, \quad r^* = \frac{r}{b}, \quad \eta^* = \frac{a}{b}, \quad \delta^*(\cdot) = b\delta(\cdot), \tag{5}$$

$$\gamma^* = \gamma b^2\sqrt{\frac{\rho h}{D}}, \quad t^* = \frac{t}{b^2}\sqrt{\frac{D}{\rho h}}, \quad \Omega^* = \Omega b^2\sqrt{\frac{\rho h}{D}}, \tag{6}$$

$$\sigma_r^* = \frac{hb^2}{D}\sigma_r, \quad \sigma_r^* = \frac{hb^2}{D}\sigma_r, \quad \epsilon^* = \frac{hb^2}{D}\epsilon \tag{7}$$

and operators

$$L^* \equiv -\left[\frac{\partial}{\partial r^*}\left(r^*\sigma_r^*\frac{\partial}{\partial r^*}\right)+\frac{\partial}{\partial\theta}\left(\frac{1}{r^*}\sigma_\theta^*\frac{\partial}{\partial\theta}\right)\right] \tag{8}$$

$$\hat{L}_k^* \equiv -\left[\frac{\partial}{\partial r^*}\left(r^*\hat{\sigma}_{rk}\frac{\partial}{\partial r^*}+\hat{\sigma}_{r\theta k}\frac{\partial}{\partial\theta}\right)+\frac{\partial}{\partial\theta}\left(\hat{\sigma}_{r\theta k}\frac{\partial}{\partial r^*}+\frac{1}{r^*}\hat{\sigma}_{\theta k}\frac{\partial}{\partial\theta}\right)\right]. \tag{9}$$

After substituting Eqs. (5)–(9) into Eqs. (3) and (4), and dropping the asterisks in what follows for brevity, Eq. (3) can be rewritten in the dimensionless operator form

$$M\frac{\partial^2 w}{\partial t^2}+G\frac{\partial w}{\partial t}+(K+\hat{K})w=0 \tag{10}$$

where

$$M \equiv 1, \quad G \equiv 2\Omega\frac{\partial}{\partial\theta}, \quad K \equiv \Omega^2\frac{\partial^2}{\partial\theta^2}+\nabla^4+L,$$

$$\hat{K} \equiv \epsilon\cos\gamma t\sum_{k=0}^{\infty} f_k\left[\hat{L}_k+\delta(r-1)\cos k\theta\frac{\partial}{\partial r}\right].$$

Equation (10) can also be cast in the first-order operator form

$$(\mathbf{A}+\hat{\mathbf{A}})\frac{\partial\mathbf{x}}{\partial t}-(\mathbf{B}+\hat{\mathbf{B}})\mathbf{x}=0 \tag{11}$$

by defining the state vector

$$\mathbf{x} \equiv \begin{Bmatrix}\dfrac{\partial w}{\partial t}\\ w\end{Bmatrix}$$

and the matrix differential operators

$$\mathbf{A} \equiv \begin{bmatrix}M & 0\\ 0 & K\end{bmatrix}, \quad \hat{\mathbf{A}} \equiv \begin{bmatrix}0 & 0\\ 0 & \hat{K}\end{bmatrix},$$

$$\mathbf{B} \equiv \begin{bmatrix}-G & -K\\ K & 0\end{bmatrix}, \quad \hat{\mathbf{B}} \equiv \begin{bmatrix}0 & -\hat{K}\\ \hat{K} & 0\end{bmatrix}.$$

For a freely spinning disk (i.e., in the absence of the edge load), Eq. (10) can be reduced to

$$M\frac{\partial^2 w}{\partial t^2} + G\frac{\partial w}{\partial t} + Kw = 0 \tag{12}$$

Since M and K are symmetric and G is skew, Eq. (12) is a standard gyroscopic equation. The eigenvalues of the $e^{\lambda t}$ time-reduced form of Eq. (12), together with the associated homogeneous boundary conditions, are purely imaginary and occur in complex conjugate pairs, i.e., $\lambda_{mn} = i\omega_{mn}$, where ω_{mn} is real. The eigenfunction corresponding to λ_{mn} is in general complex and assumes the form

$$w_{mn} = R_{mn}(r)e^{in\theta}. \tag{13}$$

R_{mn} is a real-valued function of r. The natural frequency corresponding to eigenfunction $\bar{w}_{mn}$ is $\bar{\lambda}_{mn}$, where overbar means complex conjugate. It is noted that $\bar{w}_{mn} = w_{m,-n}$. If we consider only positive natural frequency, then w_{mn} in Eq. (13) with positive n is a backward traveling wave with n nodal diameters and m nodal circles, which is also denoted by $(m, n)_b$. Similarly, w_{mn} with negative n is a forward traveling wave $(m, -n)_f$. The critical speed Ω_c for the mode (m, n) is defined as the rotation speed at which ω_{mn} of the backward traveling wave $(m, n)_b$ becomes zero. For Ω greater than Ω_c, this mode is a forward traveling wave, and is called a "reflected wave," denoted by $(m, -n)_r$. Figure 2 shows the dimensionless natural frequencies ω_{mn} of a freely spinning disk as functions of dimensionless rotation speed Ω. For simplicity, only the modes with less than four nodal diameters are shown here. The material properties of the disk used in the calculation are: $\rho = 7.84 \times 10^3$ kg/m^3, $E = 203 \times 10^9$ N/m^2, $\nu = 0.27$, $h = 1.02$ mm (0.04 in.), $a =$ 101.6 mm (4 in.), and $b = 203.2$ mm (8 in.). The natural frequencies of the modes with nodal circle(s) are beyond the range of Fig. 2.

Discretization

It has been shown in Chen and Bogy (1992) that for a freely spinning disk, the orthogonality relations among the eigenfunctions can be written as follows:

$$\langle \mathbf{x}_{mn}, \mathbf{A}\mathbf{x}_{pq}\rangle = 0, \quad \langle \mathbf{x}_{mn}, \mathbf{B}\mathbf{x}_{pq}\rangle = 0 \quad \text{if} \quad \lambda_{mn} \neq \lambda_{pq} \tag{14}$$

where the inner product between two vectors $\mathbf{x}_{mn}$ and $\mathbf{x}_{pq}$ is defined as

$$\langle \mathbf{x}_{mn}, \mathbf{x}_{pq}\rangle = \int_0^{2\pi}\int_\eta^1 \bar{\mathbf{x}}_{mn}^T \mathbf{x}_{pq} r dr d\theta. \tag{15}$$

$\mathbf{x}_{mn}^T$ is the transpose of the state vector $\mathbf{x}_{mn}$. Although Chen and Bogy (1992) only showed orthogonality properties among eigenfunctions with distinct eigenvalues for general gyroscopic systems, orthogonal relations still exist when the eigenmodes happen to be degenerate in the case of a freely spinning disk. It is noted that while eigenfunctions w_{mn} and $\bar{w}_{mn}$ represent the same mode of vibration physically, $\mathbf{x}_{mn}$ and $\bar{\mathbf{x}}_{mn}$ are two orthogonal state vectors in the inner product space defined by Eq. (15).

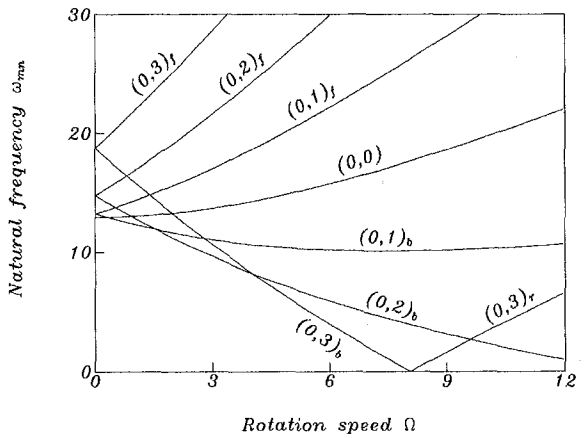

Fig. 2 Dimensionless natural frequency ω_{mn} versus dimensionless rotation speed Ω for a freely spinning disk

Since a closed-form solution for Eq. (11) does not exist in general, we use an expansion in terms of finite number of eigenfunctions of the freely spinning disk to approximate the true solution of Eq. (11),

$$\mathbf{x}(r, \theta; t) \approx \sum_{p=0}^{N_1}\sum_{q=-N_2}^{N_2} c_{pq}(t)\mathbf{x}_{pq}(r, \theta). \tag{16}$$

N_1 and N_2 are the maximum numbers of nodal circles and nodal diameters, respectively, of the modes used in the expansion. Scalar amplitude function $c_{pq}(t)$ is in general complex. It is noted that the right-hand side of Eq. (16) involves both modes $\mathbf{x}_{pq}$ and $\bar{\mathbf{x}}_{pq}$. The validity of expansion (16) has been confirmed in Chen (1996), in which the eigenvalues of a spinning disk under time-invariant space-fixed edge loads are calculated and compared both by expansion (16) and an independent finite element scheme. Substituting Eq. (16) into (11) and taking the inner product between $\mathbf{x}_{mn}$ and both sides of Eq. (11), with use of the orthogonality properties (14), we obtain a system of generalized Hill's equations in the first order form,

$$\frac{dc_{mn}}{dt} - i\omega_{mn}c_{mn} + \epsilon\cos\gamma t \times \sum_{k=0}^{\infty}\sum_{p=0}^{N_1}\sum_{q=-N_2}^{N_2}\left[\frac{\hat{A}_{pq(k)}^{mn}}{A_{mn}^{mn}}\frac{dc_{pq}}{dt} - \frac{\hat{B}_{pq(k)}^{mn}}{A_{mn}^{mn}}c_{pq}\right] = 0 \tag{17}$$

where

$$A_{mn}^{mn} = 4\pi\omega_{mn}(\omega_{mn} + n\Omega)\int_\eta^1 R_{mn}^2(r) r dr. \tag{18}$$

The physical meaning of the above discretization procedure is to force the error function of the approximation (16) to be orthogonal to all eigenfunctions $\mathbf{x}_{pq}(r, \theta)$ used in the expansion. Therefore, the above discretization technique falls into the category of the so-called Galerkin's method. It can be shown that constant A_{mn}^{mn} is a positive real number when the mode (m, n) is a nonreflected wave, and it is negative when (m, n) is a reflected wave (Chen and Bogy, 1992). When $n - q \neq \pm k$, $\hat{A}_{pq(k)}^{mn} = \hat{B}_{pq(k)}^{mn} = 0$. On the other hand, when $n - q = \pm k$, we obtain

$$\hat{A}_{pq(k)}^{mn} = \hat{A}_{mn(k)}^{pq} = \alpha_k\int_\eta^1\left[r\tilde{\sigma}_{rk}\frac{dR_{mn}}{dr}\frac{dR_{pq}}{dr} + q\left(n\frac{\tilde{\sigma}_{\theta k}}{r} - \frac{d\tilde{\sigma}_{r\theta k}}{dr}\right)R_{mn}R_{pq} - (n+q)\tilde{\sigma}_{r\theta k}R_{mn}\frac{dR_{pq}}{dr}\right]dr \tag{19}$$

$$\hat{B}_{pq(k)}^{mn} = i(\omega_{mn} + \omega_{pq})\hat{A}_{pq(k)}^{mn} \tag{20}$$

where $\alpha_0 = 2\pi f_0$, and $\alpha_k = \pi f_k$ when $k \neq 0$. In summary, the coefficients $\hat{A}_{pq(k)}^{mn}$ and $\hat{B}_{pq(k)}^{mn}$ are determined by the eigenfunctions w_{mn} and w_{pq}, and are affected only by the specific Fourier component $\cos k\theta$ of the edge loads with $n - q = \pm k$.

It is in general difficult to find the closed-form expression for the real-valued function $R_{mn}(r)$ when the disk is spinning. However, it is possible to obtain the values of this function at discrete radial points by a finite element method (Ono and Maeno, 1987). The matrices A_{mn}^{mn}, $\hat{A}_{pq}^{mn}$, and $\hat{B}_{pq}^{mn}$ in Eqs. (18)–(20) can then be obtained through numerical integration.

Perturbation Technique

In this section we apply the method of multiple scale to determine the conditions for parametric resonance to occur. The methodology of this perturbation technique has been described and applied by Nayfeh and Mook (1977) to a system of second-order nongyroscopic equations. In this section we extend this methodology to solve a system of gyroscopic equations in the first-order form.

The method of multiple scale assumes an expansion of the form

$$c_{mn}(t) = c_{mn}^{(0)}(t, T_1) + \epsilon c_{mn}^{(1)}(t, T_1) + O(\epsilon^2) \tag{21}$$

where $T_1 \equiv \epsilon t$. In Eq. (21) the amplitude parameter ϵ is assumed to be smaller than 1. Substituting (21) into (17) and equating coefficients of like powers of ϵ yield

$$\epsilon^0: \quad D_0 c_{mn}^{(0)} - i\omega_{mn} c_{mn}^{(0)} = 0 \tag{22}$$

$$\epsilon^1: \quad D_0 c_{mn}^{(1)} - i\omega_{mn} c_{mn}^{(1)} = -D_1 c_{mn}^{(0)} - \cos \gamma t \sum_{k=0}^{\infty} \sum_{p=0}^{N_1} \sum_{q=-N_2}^{N_2} \frac{\hat{A}_{pq(k)}^{mn}}{A_{mn}^{mn}} D_0 c_{pq}^{(0)} - \frac{\hat{B}_{pq(k)}^{mn}}{A_{mn}^{mn}} c_{pq}^{(0)} \tag{23}$$

where $D_0 \equiv (\partial/\partial t)$, and $D_1 \equiv (\partial/\partial T_1)$. The general solution of Eq. (22) can be written in the form

$$c_{mn}^{(0)} = H_{mn}(T_1) e^{i\omega_{mn} T_0}. \tag{24}$$

Substituting (24) into (23) yields

$$D_0 c_{mn}^{(1)} - i\omega_{mn} c_{mn}^{(1)} = -D_1 H_{mn} e^{i\omega_{mn} T_0} + \frac{\omega_{mn}}{2} \sum_{k=0}^{\infty} \sum_{p=0}^{N_1} \sum_{q=-N_2}^{N_2} \frac{\hat{A}_{pq(k)}^{mn}}{A_{mn}^{mn}} H_{pq} [e^{i(\omega_{pq}+\gamma)T_0} + e^{i(\omega_{pq}-\gamma)T_0}] \tag{25}$$

Combination Resonance at $\gamma = \omega_{rs} + \omega_{uv} + \epsilon\zeta$. In the case when γ is near $\omega_{rs} + \omega_{uv}$, we assume that $\gamma = \omega_{rs} + \omega_{uv} + \epsilon\zeta$, where ζ is a detuning parameter. The secular terms in Eq. (25) are eliminated if

$$D_1 H_{rs} - i\omega_{rs} \frac{\sum_{k=0}^{\infty} \hat{A}_{u,-v(k)}^{rs}}{2A_{rs}^{rs}} \bar{H}_{uv} e^{i\zeta T_1} = 0 \tag{26}$$

and

$$D_1 H_{uv} - i\omega_{uv} \frac{\sum_{k=0}^{\infty} \hat{A}_{r,-s(k)}^{uv}}{2A_{uv}^{uv}} \bar{H}_{rs} e^{i\zeta T_1} = 0 \tag{27}$$

Equations (26) and (27) admit nontrivial solutions having the form

$$H_{rs} = h_{rs} e^{-i\lambda T_1} \quad \text{and} \quad H_{uv} = h_{uv} e^{i(\bar{\lambda}+\zeta)T_1} \tag{28}$$

where h_{rs} and h_{uv} are complex constants, and

$$\lambda = \frac{-\zeta \pm \sqrt{\zeta^2 - \Lambda_{uv}^{rs}}}{2} \tag{29}$$

where

$$\Lambda_{uv}^{rs} = \frac{\omega_{rs}\omega_{uv} \left[\sum_{k=0}^{\infty} \hat{A}_{u,-v(k)}^{rs}\right]^2}{A_{rs}^{rs} A_{uv}^{uv}}. \tag{30}$$

It follows from Eq. (29) that the solution of Eq. (17) is bounded if and only if

$$\zeta^2 \geq \Lambda_{uv}^{rs} \tag{31}$$

On the other hand, combination resonance may occur when $\zeta^2 < \Lambda_{uv}^{rs}$. Frequency $\omega_{rs} + \omega_{uv}$ is called the center frequency and $\sqrt{\Lambda_{uv}^{rs}}$ is called the width parameter of the parametric resonance.

Single-Mode Resonance at $\gamma = 2\omega_{rs} + \epsilon\zeta$. In this case the secular term in Eq. (25) is eliminated if

$$D_1 H_{rs} - i\omega_{rs} \frac{\sum_{k=0}^{\infty} \hat{A}_{r,-s(k)}^{rs}}{2A_{rs}^{rs}} \bar{H}_{rs} e^{i\zeta T_1} = 0 \tag{32}$$

Equation (32) admits nontrivial solution having the form

$$H_{rs} = [\alpha(T_1) + i\beta(T_1)] e^{(i/2)\zeta T_1}. \tag{33}$$

Substituting Eq. (33) into (32), equating the real and imaginary parts to zero, and evoking the condition for $\alpha(T_1)$ and $\beta(T_1)$ to be bounded result in the condition

$$\zeta^2 \geq \Lambda_{rs}^{rs} \tag{34}$$

where

$$\Lambda_{rs}^{rs} = \left[\frac{\omega_{rs} \sum_{k=0}^{\infty} \hat{A}_{r,-s(k)}^{rs}}{A_{rs}^{rs}}\right]^2 \geq 0. \tag{35}$$

Consequently, single-mode parametric resonance may occur if the summation $\sum_{k=0}^{\infty} \hat{A}_{r,-s(k)}^{rs}$ does not vanish. It is noted that Eq. (35) can also be obtained by substituting (u, v) by (r, s) directly in Eq. (30).

Typical Edge Loading

Concentrated Edge Load. We first consider the case when the spinning disk is subjected to a space-fixed concentrated edge load. In this case the Fourier decomposition of the edge load would include all the harmonics of cos $k\theta$, and the summation $\sum_{k=0}^{\infty} \hat{A}_{u,-v(k)}^{rs}$ in Eq. (30) reduces to a single nonzero term $\hat{A}_{u,-v(k)}^{rs}$, where $s + v = \pm k$. In other words, for any two modes (r, s) and (u, v), there always exists a specific Fourier component which renders the summation $\sum_{k=0}^{\infty} \hat{A}_{u,-v(k)}^{rs}$ nonzero. Bearing the relation $\omega_{mn} = -\omega_{m,-n}$ in mind and speaking of only positive natural frequencies, we can conclude that combination resonance of the sum type occurs when both modes are nonreflected or both modes are reflected. On the other hand, combination resonance of the difference type can occur only when one mode is reflected and the other is nonreflected. Single mode parametric resonance can occur for any mode, reflected or nonreflected.

The center frequency and the width parameter of a spinning disk under a pulsating concentrated edge load are shown in Fig. 3. Solid lines represent the single-mode parametric resonance, while dashed lines and dotted lines represent the cases of combination resonance of the sum type and difference type, respectively. In the frequency range of Fig. 3 only the modes with zero nodal circle contribute to the parametric resonance. The mode labels in Fig. 3 are simplified by neglecting the number of nodal circle. For instance, $0 + 2_f$ represents the combination resonance of the sum type involving modes (0, 0) and $(0, 2)_f$, and $2_b - 3_r$ represents the combination resonance of the difference type involving modes $(0, 2)_b$ and $(0, 3)_r$. It can be seen from Fig. 3 that the rotation speed tends to squeeze the width of parametric resonance region.

In the special case when the excitation frequency γ approaches zero, which corresponds to the case of constant con-

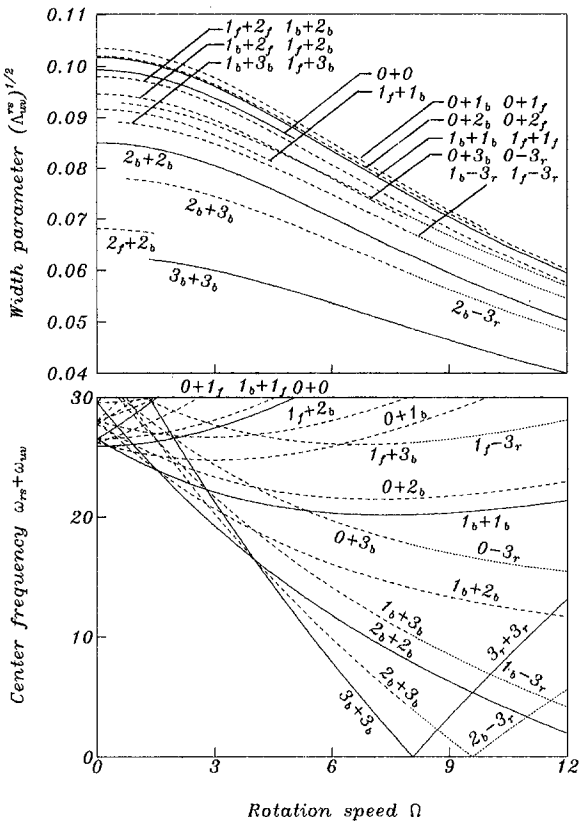

Fig. 3 Center frequencies and width parameters of a spinning disk under a space-fixed pulsating concentrated edge load. Solid lines represent the single mode parametric resonance. Dashed and dotted lines represent the combination resonance of the sum type and the difference type, respectively.

centrated edge load, we can see from Fig. 3 that there exist two rotation speeds at which parametric resonance can occur. The rotation speed at which the solid line labeled $3_b + 3_b$ intersects the horizontal line $\omega_{rs} + \omega_{uv} = 0$ corresponds to the first critical speed. Therefore, the divergence instability reported by Chen (1994) can be considered as a limit case of single mode parametric resonance. On the other hand, the rotation speed at which the dotted line labeled $2_b - 3_r$ intersects the line $\omega_{rs} + \omega_{uv} = 0$ is a speed at which the backward wave $(0, 2)_b$ and reflected wave $(0, 3)_r$ become degenerate. Therefore, the flutter instability reported by Chen (1994) can be considered as a limit case of combination resonance of the difference type.

Uniform Edge Load. In this case the summation $\sum_{k=0}^{\infty} \hat{A}^{rs}_{u,-\nu(k)}$ in Eq. (30) reduces to $\hat{A}^{rs}_{u,-\nu(0)}$, and is equal to zero unless $s = -\nu$. Consequently, we can conclude that combination resonance of the sum type occurs only when both modes have the same number of nodal diameters, and one of them is a forward wave while the other is a backward wave. On the other hand, combination resonance of the difference type occurs when both modes have the same number of nodal diameters, and one mode is a backward wave while the other is a reflected wave. From Eq. (35) we can see that single-mode parametric resonance is possible only for zero-nodal diameter modes. Therefore, the center frequency and width parameter graphs for a spinning disk under uniform edge load can be obtained by retaining only the dashed curve $1_f + 1_b$ and solid curve 0 + 0 in Fig. 3.

Another way to look at the above problem is to fix the coordinate system onto the spinning disk. Since the loading is uniform circumferentially, it appears no difference to both the stationary and the spinning coordinate systems. To an observer spinning along with the disk, there is only one natural frequency for the (0, 1) mode, which is the average of the natural frequencies of modes $(0, 1)_f$ and $(0, 1)_b$ as observed by another observer in the stationary coordinate system. Therefore, the curves $1_f + 1_b$ and 0 + 0 in Fig. 3 represent the single mode parametric resonance involving modes (0, 1) and (0, 0), respectively, as observed by a spinning observer.

As the rotation speed Ω approaches zero, the natural frequency of the forward wave $(r, s)_f$ and the backward wave $(r, s)_b$ coincide. Consequently, single mode parametric resonance occurs for each mode when a stationary disk is under uniform loading. Furthermore, combination resonance of the sum type can occur whenever two modes have the same number of nodal diameters.

Conclusions

Dynamic stability of a spinning annular disk under periodically varying in-plane loading on the outer rim is studied analytically. The equation of motion is gyroscopic due to relative motion between the spinning disk and the space-fixed edge loading. The differential equation of motion is first discretized into a system of generalized Hill's equations of the first-order form. Conventional method of multiple scale is extended to treat the system of gyroscopic equations. The results show that combination resonance is possible only when there exists a specific Fourier component cos $k\theta$ in the edge load, where k equals the sum of the number of nodal diameters of these two modes. Sum type resonance occurs when both modes are nonreflected or both modes are reflected. On the other hand, difference type resonance occurs when one mode is reflected and the other is nonreflected.

References

Carlin, J. F., Appl, F. C., Bridwell, H. C., and Dubois, R. P., 1975, "Effects of Tensioning on Buckling and Vibration of Circular Saw Blades," ASME *Journal of Engineering for Industry,* Vol. 2, pp. 37–48.

Chen, J.-S., 1994, "Stability Analysis of a Spinning Elastic Disk Under a Stationary Concentrated Edge Load," ASME JOURNAL OF APPLIED MECHANICS, Vol. 61, pp. 788–792.

Chen, J.-S., 1996, "Vibration and Stability of a Spinning Disk Under Stationary Distributed Edge Loads," ASME JOURNAL OF APPLIED MECHANICS, Vol. 63, pp. 439–444.

Chen, J.-S., and Bogy, D. B., 1992, "Effects of Load Parameters on the Natural Frequencies and Stability of a Flexible Spinning Disk With a Stationary Load System," ASME JOURNAL OF APPLIED MECHANICS, Vol. 59, pp. S230–S235.

Coker, E. G., and Filon, L. N. G., 1957, *A Treatise on Photo-Elasticity,* Cambridge University Press, London, U.K.

Nayfeh, A. H., and Mook, D. T., 1977, "Parametric Excitations of Linear Systems Having Many Degrees of Freedom," *Journal of Acoustical Society of America,* Vol. 62, pp. 375–381.

Ono, K., and Maeno, T., 1987, "Theoretical and Experimental Investigation on Dynamic Characteristics of a 3.5-Inch Flexible Disk Due to a Point Contact Head," *Tribology and Mechanics of Magnetic Storage Systems,* Vol. 3, SP.21 (STLE), pp. 144–151.

Radcliffe, C. J., and Mote, C. D., Jr., 1977, "Stability of Stationary and Rotating Discs Under Edge Load," *International Journal of Mechanical Sciences,* Vol. 19, pp. 567–574.

Tani, J., and Nakamura, T., 1978, "Dynamic Stability of Annular Plates Under Periodic Radial Loads," *Journal of Acoustical Society of America,* Vol. 64, pp. 827–831.

Tani, J., and Nakamura, T., 1980, "Dynamic Stability of Annular Plates Under Pulsating Torsion," ASME JOURNAL OF APPLIED MECHANICS, Vol. 47, pp. 595–600.

Zajaczkowski, J., 1983, "Stability of Transverse Vibration of a Circular Plate Subjected to a Periodically Varying Torque," *Journal of Sound and Vibration,* Vol. 89, pp. 273–286.